3-(3,4-Dihydroisoquinolin-2(1H)-ylsulfonyl)benzoic Acids: Highly Potent and Selective Inhibitors of the Type 5 17-β-Hydroxysteroid Dehydrogenase AKR1C3

Stephen M. F. Jamieson,[†] Darby G. Brooke,[†] Daniel Heinrich,[†] Graham J. Atwell,[†] Shevan Silva,[†] Emma J. Hamilton,[†] Andrew P. Turnbull,[§] Laurent J. M. Rigoreau,[‡] Elisabeth Trivier,[‡] Christelle Soudy,[‡] Sharon S. Samlal,[‡] Paul J. Owen,[‡] Ewald Schroeder,[‡] Tony Raynham,[‡] Jack U. Flanagan,[†] and William A. Denny*,[†]

[†]Auckland Cancer Society Research Centre, The University of Auckland, Private Bag 92019, Auckland 1142, New Zealand
[§]Cancer Research Technology Ltd, Birkbeck College, University of London, London, U.K.
[‡]Cancer Research Technology Ltd, Wolfson Institute for Biomedical Research, The Cruciform Building, Gower Street, London WC1E 6BT, U.K.

S Supporting Information

ABSTRACT: A high-throughput screen identified 3-(3,4-dihydroisoquinolin-2(1H)-ylsulfonyl)benzoic acid as a novel, highly potent (low nM), and isoform-selective (1500-fold) inhibitor of aldo-keto reductase AKR1C3: a target of interest in both breast and prostate cancer. Crystal structure studies showed that the carboxylate group occupies the oxyanion hole in the enzyme, while the sulfonamide provides the correct twist to allow the dihydroisoquinoline to bind in an adjacent hydrophobic pocket. SAR studies around this lead showed that the positioning of the carboxylate was critical, although it could be substituted by acid isosteres and amides. Small substituents on the dihydroisoquinoline gave improvements in potency. A set of "reverse sulfonamides" showed a 12-fold preference for the R stereoisomer. The compounds showed good cellular potency, as measured by inhibition of AKR1C3 metabolism of a known dinitrobenzamide substrate, with a broad rank order between enzymic and cellular activity, but amide analogues were more effective than predicted by the cellular assay.

R = Me, halogen, OMe, OH, NH$_2$, NO$_2$, CN
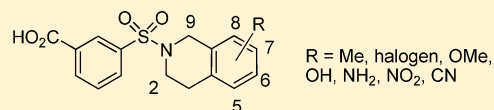
The type 5 17-β-hydroxysteroid dehydrogenase is a member of the aldo-keto reductase (AKR) superfamily of enzymes,[1] where it is also known as AKR1C3. It is expressed in the human prostate and mammary gland, where it is responsible for reducing androst-4-ene-3,17-dione, estrone, and progesterone to, respectively, testosterone, 17β-estradiol, and 20α-hydroxprogesterone.[2] This production of growth-stimulatory steroid hormones by AKR1C3 makes it a target of interest in both breast and prostate cancer. AKR1C3 is also known as prostaglandin F$_2$ synthase,[3] as it transforms PGH$_2$ to PGF$_{2\alpha}$ and PGD$_2$ to 9α,11β-PGF$_{2\alpha}$, thus diverting PGD$_2$ (**1**) from the PGJ$_2$ pathway that governs cellular differentiation,[4] making it also a potential drug target for some leukemias. AKR1C3 has also been reported to metabolize some drugs; notably, inactivating the topoisomerase poison doxorubicin[5] and catalyzing the aerobic activation of the hypoxia prodrug PR-104.[6]

There are three closely related isoforms of AKR1C3 (AKR1C1, AKR1C2, and AKR1C4), which are also involved in steroid hormone metabolism. These enzymes, in particular AKR1C1 and AKR1C2, are not ideal drug targets, since they can prevent androgen signaling and cell proliferation by catalyzing the reduction of the potent androgen 5α-dihydrotestosterone to 5α-androstane-3β,17β-diol and 5α-androstane-3α,17β-diol, respectively.[7] AKR1C3 has weak 5α-

dihydrotestosterone reductase activity, but with 100-fold less catalytic efficiency than the reduction of PGD$_2$.[8]

Among the classes of compounds studied[9,10] as potential competitive inhibitors of the AKR1C family of enzymes are structural mimics of prostaglandin D$_2$. In this class are compounds such as the plant stress hormone jasmonic acid (**2**), which shows K_i values for the inhibition of AKR1C1-4 of 106, 18, 162, and 37 μM, respectively.[11] Simpler analogues such as the benzylidenecyclopentanone **3** also showed modest inhibitory activity (IC$_{50}$ values approximately 35 μM for AKR1C-1 and -3).[12]

Based on kinetic data, it was suggested that the reductive reactions promoted by AKR1C3 proceed through an oxyanion transition state and that steroid carboxylates might be suitable competitive inhibitors.[2] A later study[13] showed this to be the case, with (for example) the cholanic acid analogue (**4**) showing IC$_{50}$ values of 14.0, 0.04, and 1.02 μM, respectively, for inhibition of AKR1C1, -2, and -3, with high selectivity with respect to inhibition of COX1 and COX2 (IC$_{50}$ values > 250 μM). The crystal structure of AKR1C3 complexed with the flavanoid rutin (**5**)[14] (PBD 1RY8) showed H-bond formation with the conserved Y55 and H117 residues that constitute the

Table 1. Selected Known Inhibitors of AKR1C3

no.	compd[a]	AKR isoform IC$_{50}$ (μM)[b]			
		1C1	1C2	1C3	1C4
11	flufenamic acid	2.64 ± 0.68	3.14 ± 0.50	0.41 ± 0.15	>100
12	indomethacin	>100	>100	0.73 ± 0.16	>100
13	naproxen	>100	31.3 ± 16.3	1.1 ± 0.47	>100
14	meclofenamic acid	3.16 ± 1.18	8.74 ± 4.29	0.54 ± 0.14	>100
15	S(+)-ibuprofen	>100	42.4 ± 21.0	32.7 ± 12.7	>100
16	flurbiprofen	>100	32.5 ± 19.6	1.56 ± 0.83	>100

[a]See Figure 1 for structures. [b]IC$_{50}$ values were determined using a competitive fluorescence assay; see Experimental Section.

"oxyanion hole". The related compound 2′-hydroxyflavanone (**6**) showed good *in vitro* potency for AKR1C3 (IC$_{50}$ 0.10 μM, with 62-fold selectivity over AKR1C2).[15] Cinnamic acids, which are flavonoid precursors, also show some inhibitory activity; the bis(cinnamic acid) baccharin (**7**) has an IC$_{50}$ of 0.11 μM and high selectivity for AKR1C3.[16]

A series of substituted *N*-phenylanthranilic acids also showed good AKR1C3 potencies, with high selectivity over COX enzymes.[13] For example, **8** had IC$_{50}$ values of 4.0, 0.96, 0.39, 33, and 225 μM, respectively, for the inhibition of AKR1C-1, -2, and -3 and COX1 and COX2. Studies[13,17] on a series of substituted 3-(phenylamino)benzoic acids showed that AKR1C3 inhibitory activity correlated positively with the electron-withdrawing capability of 4-substituents (which affects the carboxylate pK_a), e.g, compounds **9** and **10**.

The widespread observation that nonsteroidal anti-inflammatory drugs (NSAIDs) appear to protect against a variety of cancers, including prostate carcinoma, gastrointestinal tumors, and leukemia,[18] prompted the suggestion[19] that inhibition of AKR1C3 might be a contributing mechanism of action. Crystal structures of the NSAIDs flufenamic acid (**11**) and indomethacin (**12**) with AKR1C3 show that the carboxylate of the former occupies the oxyanion hole, but in the latter, the ketone oxygen is in close proximity to this binding site.[19] Indomethacin was an effective inhibitor of AKR1C3 (IC$_{50}$ 2.3 μM), with a 20−40-fold selectivity over AKR1C1 and -C2. Several other known NSAIDS, including naproxen, (**13**), meclofenamic acid (**14**), S(+)-ibuprofen (**15**), and flurbiprofen (**16**) are also known[20] to have AKR1C isoform activity (Table 1).

In a project seeking novel, more potent, and highly selective inhibitors of AKR1C3, we conducted a high-throughput screen. AKR1C3 was cloned in an *E. coli* expression vector with a N-terminal His tag for assay development. The assay used a fluorescent readout (probe **5**; see Supporting Information for structure). A screen of 99,000 compounds from an in-house library gave 8000 primary hits, which were trimmed to 960 by removal of kinase library compounds and by inspection. Generation of 5-point IC$_{50}$ values gave 187 compounds with estimated activities of <1 μM, from which 3-(3,4-dihydroisoquinolin-2(1*H*)-ylsulfonyl)benzoic acid (**17**) (Table 2) was selected as a lead. In this paper we discuss the development of this lead, including the development of structure−activity relationships (SAR) and a crystal structure-derived model of the binding of the class to AKR1C3.

■ **CHEMISTRY**

Compounds **17**−**24** of Table 2 were prepared by direct coupling of sulfonyl chloride **95** and the required amines (Scheme 1A). Compound **24** of Table 2 was prepared by a
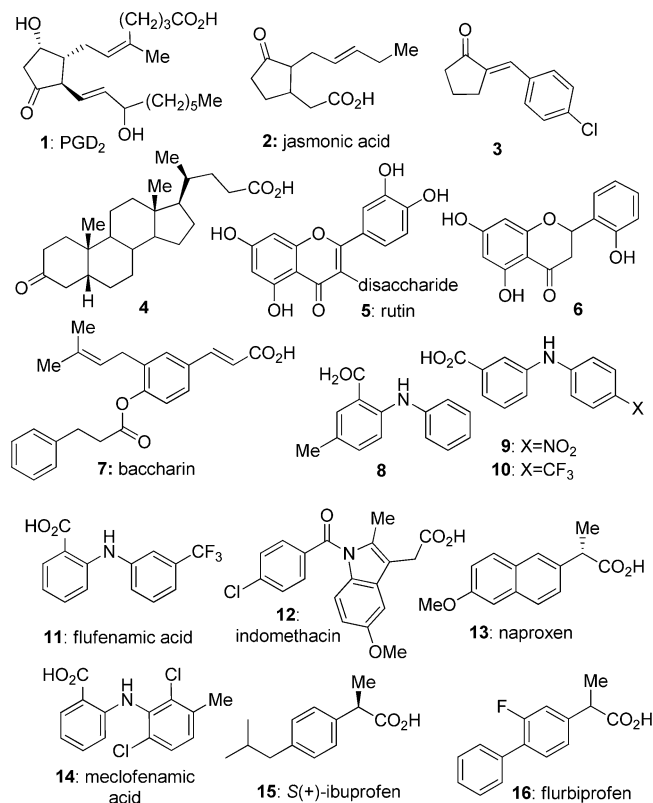
Figure 1.

literature method.[21] Compound **17** of Table 4 was previously reported as an intermediate in the synthesis of a series of PPARδ partial agonists.[22]

Energy minimization was performed with SZYBKI using the MM-PBSA implicit solvent model. For the free ligand, minimization was performed with a dielectric constant of 80 and a microcavitation term of 0.25. RMSD values are reported in angstroms, and RMSD$_{[protein]}$ is the RMSD after ligand minimization within the AKR1C3 active site. $E_{[Bound]}$ is the ligand energy in the conformation minimized in the active site, while $E_{[Free]}$ is the energy after minimization of that conformation in the absence of protein. $\Delta E_{[Bound−Free]}$ is the difference between the two energies. Energy is reported as kilocalories per mole. RMSD[Bound−Free] is the difference in angstroms between the two conformations. LPE is the Ligand−Protein energy reported by SZYBKI.

The majority of the compounds of Table 3 were prepared by coupling of sulfonyl chloride **96** with commercially available or previously reported substituted 1,2,3,4-tetrahydroisoquinolines (**96a**−**x**) (Scheme 1A). Reaction of the 7-nitrile **51** with NaN$_3$ gave the tetrazole **45**. Suzuki coupling of iodide **50** with

Table 2. Variation of the Dihydroisoquinoline Unit of 17

No	R	IC$_{50}$ (μM)[a]				
		1C1	1C2	1C3	1C4	HCT-116[b]
17		20.3±3.8	>30	0.013±0.003	>30	0.027±0.002
18		>30	>30	0.39±0.06	>30	>1
19		>30	>30	0.025±0.008	>30	0.034
20		6.61±1.56	>30	0.21±0.06	>30	>1
21		3.89±0.58	>30	0.047±0.018	>30	0.884
22		>30	>30	0.20±0.03	>30	>1
23		>30	>30	0.60±0.01	>30	
24[c]		0.83±0.27	>30	0.068±0.025	>30	0.407

[a]IC$_{50}$ values were determined using a competitive fluorescence assay; see Experimental Section. [b]Concentration of drug to inhibit the conversion of nitroaromatic prodrug PR-104A to the hydroxylamine in HCT-116 cells engineered to overexpress AKR1C3, as determined by LC-MS/MS; see Experimental Section. [c]Reference 21.

Scheme 1. Compounds of Tables 2 and 3[a]

[a]Reagents and conditions: (i) K$_2$CO$_3$ or Et$_3$N, THF/water or Me$_2$CO, N$_2$ atmosphere, 0−20 °C over 3−72 h; (ii) NaN$_3$, NH$_4$Cl, DMF, 120 °C, 170 h; (iii) Pd(PPh$_3$)$_2$Cl$_2$, piperidine, 20 °C, 12 h; (iv) Cs$_2$CO$_3$, MeOH, 20 °C, 100 min; (v) Pd(PPh$_3$)$_4$, CuI, TMS-CCH, DIPE, 20 °C, 48 h; (vi) 2,4-dichloro-5,5-dimethylhydantoin, MeCN/AcOH/water, 0−20 °C, 110 min; (vii) LiOH, MeOH, 20 °C, 80 min.

(trimethylsilyl)acetylene (**97**) gave the adduct **98**, which was deprotected with Cs$_2$CO$_3$ to give **43** (Scheme 1B). Similar reaction of **50** with 1-ethynyl-4-(trifluoromethoxy)benzene (**99**) gave **44** directly. Methyl 5-(chlorosulfonyl)nicotinate (**101**) for the synthesis of **55** was prepared from methyl 5-mercaptonicotinate (**100**) by the method of Isabel et al.,[23,24] except the last oxychlorination was carried out under conditions developed by Pu et al.[25] Coupling of **99b** with tetrahydroisoquinoline **96a** and hydrolysis of the product ester then gave **55** (Scheme 1C). Compounds **34**, **37**, **42**, and **48** of Table 3 were prepared conveniently (albeit in moderate to low yields) from the open-chain analogues **58**, **63**, **64**, and **59**, respectively (Table 6), on cyclization with methanesulfonic acid in s-trioxan (Scheme 2).

The open-chain analogues **56**−**64** of Table 5 were prepared (Scheme 2) by coupling the sulfonyl chloride **95** and substituted phenylethanamines **102a**−**h** under mild basic conditions (K$_2$CO$_3$, 35 °C) in a two-phase system in modest yields (10−50%, unoptimized).

The bulk of the compounds of Table 6 were similarly prepared (Scheme 3) by coupling of known 3-substituted benzenesulfonyl chlorides **103a**−**e** with 1,2,3,4-tetrahydroisoquinoline (**100a**). The 3-nitro analogue **66** prepared in this way was reduced to the amine **67**, and this was further reacted with ethyl 2-chloro-2-oxoacetate, and the resulting ester **104** was hydrolyzed with Cs$_2$CO$_3$ to give the oxoacetic acid **72**. The 3-nitrile **65** was treated with NaN$_3$ to give tetrazole **74** (Scheme 3A). The 3-amides **75**−**82** were prepared from the acid chloride of **17** and appropriate amines (Scheme 3B). Compound **83** was prepared by Pd-assisted coupling of 2-(4-iodophenylsulfonyl)-1,2,3,4-tetrahydroisoquinoline (**105**) and 2-pyrrolidinone (Scheme 3C).

Finally, the "reverse sulfonamides" **84**−**94** of Table 7 (Scheme 4) were constructed from known sulfonyl chlorides **106**, **107a**−**f** and known amines **108**, **109a**−**e**.

■ RESULTS AND DISCUSSION

High-Throughput Chemical Screening. Library screening against purified recombinant human AKR1C3 identified a number of compounds with IC$_{50}$ values of <200 nM, and these were tested for activity against the AKR isoforms, 1C1, 1C2, and 1C4. The frequency of hits for AKR1C3 was kept low by using a high probe 5 substrate concentration (10× K_m) at a saturating NADPH concentration. The accuracy of the biochemical assay was confirmed by generating IC$_{50}$ values for the known inhibitors (**11**−**16**), comparable with those previously published.[26]

Of several potent and selective compounds identified, the 3-(3,4-dihydroisoquinolin-2(1H)-ylsulfonyl)benzoic acid (**17**) (Table 2) represented a new class of highly potent AKR1C3 inhibitors. In repeat assays it showed an IC$_{50}$ of 0.013 ± 0.003 μM for AKR1C3, compared with 20.3 ± 3.8 μM against AKR1C1 and >30 μM against AKR1C2 and AKR1C4. This compares favorably for both potency and specificity with other known AKR1C3 inhibitors (Table 1). Representative compounds **17**, **79**, and **85** were screened for inhibition of COX-1 and COX-2 but were found to be inactive at 10 μM.

X-ray Crystallography. To understand how this potency is achieved, we determined the structure of **17** bound to AKR1C3 in the presence of oxidized NADP+, and the crystallographic

Table 3. SAR of Dihydroisoquinoline-Substituted for Inhibition of AKR Isoforms
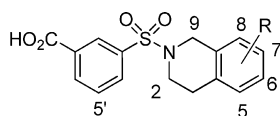
		IC_{50} $(\mu M)^a$				
no.	R	1C1	1C2	1C3	1C4	HCT-116[b]
25	9-Me	>30	>30	0.027 ± 0.022	>30	0.024
26	2-Me	>30	>30	0.0086 ± 0.0066	>30	0.176
27	5-NH$_2$	>30	>30	0.053 ± 0.047	>30	0.193
28	5-NO$_2$	24.6 ± 5.7	>30	0.0089 ± 0.0030	>30	0.029
29	5-Cl	>30	9.32 ± 3.20	0.011 ± 0.0021	>30	0.016
30	5-Br	>30	>30	0.011 ± 0.0001	>30	0.014
31	5-I	>30	>30	0.014 ± 0.008	>30	0.020
32	5-OH	25.6 ± 9.3	>30	0.016 ± 0.005	>30	0.453
33	5-OMe	>30	>30	0.016 ± 0.008	>30	0.039
34	6-Me	>30	>30	0.017 ± 0.003	>30	0.052
35	6-NO$_2$	>30	>30	0.022 ± 0.016	>30	>1
36	6-CN	17.6 ± 6.7	>30	0.029 ± 0.001	>30	
37	6-Cl	7.48 ± 0.46	>30	0.0087 ± 0.0035	>30	0.039
38	6-Br	>30	>30	0.0061 ± 0.0013	>30	0.012
39	6-I	13.9 ± 3.0	>30	0.039 ± 0.03	>30	
40	6-OH	>30	>30	0.027 ± 0.005	>30	>1
41	6-OMe	>30	>30	0.038 ± 0.016	>30	0.39 ± 0.02
42	7-Me	>30	>30	0.013 ± 0.001	>30	0.029
43	7-C≡CH	>30	>30	0.042 ± 0.034	>30	
44	7-C≡CX^c	>30	>30	1.31 ± 0.46	>30	
45	7-C-tetrazole	>30	>30	0.068 ± 0.038	9.81 ± 0.55	
46	7-NO$_2$	>30	>30	0.017 ± 0.015	>30	0.072
47	7-F	>30	>30	0.021 ± 0.009	>30	0.024
48	7-Cl	>30	>30	0.020 ± 0.019	>30	>1
49	7-Br	>30	>30	0.012 ± 0.0028	>30	0.02 ± 0.01
50	7-I	>30	>30	0.014 ± 0.004	>30	0.045
51	7-CN	>30	>30	0.034 ± 0.016	>30	0.266
52	7-OMe	>30	>30	0.029 ± 0.006	>30	
53	8-Cl	0.74 ± 0.13	12.1 ± 3.5	0.019 ± 0.014	>30	0.028
54	6,7-diOMe	>30	>30	0.16 ± 0.009	>30	>1
55	H (5̒-aza)	>30	>30	0.042 ± 0.007	>30	

^{a,b}As for Table 2. ^{c}X = 4-trifluoromethoxyphenyl.

Scheme 2. Compounds of Tables 3 and 5^a
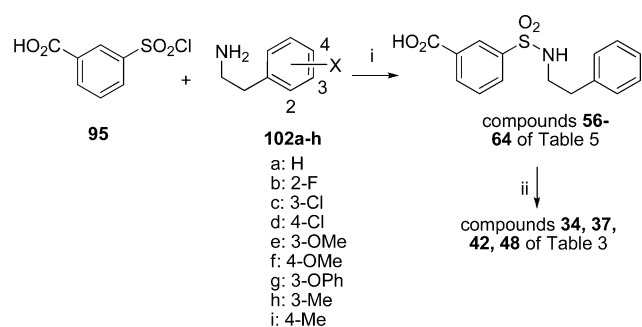
^{a}Reagents and conditions: (i) Et$_3$N or K$_2$CO$_3$, Me$_2$CO, THF, 0−20 °C, 3−90 h.

data is presented in Table S2 (see Supporting Information). The structure illustrates that the inhibitor binds in the active site cavity with its carboxylate group occupying the oxyanion hole, where it interacts with Tyr55 and His117, while the benzylic unit is located in a pocket defined by residues Tyr24, Trp227, and Phe306. The sulfonyl extends out into the central cavity, allowing the pendant tetrahydroquinoline to occupy a lipophilic cavity in the active site pocket defined by the side chains of residues Met120, Asn167, Tyr216, Phe306, Ser308, Phe111, Tyr 317, and Tyr319, and an ordered water (Figure 2A). The water molecule is located in a pocket defined by the side chain phenol OH groups of Tyr216 and Ty319 and by the carboxylate of Glu192. There are a number of ethylene glycol molecules in the structure, carried over from cryoprotecting the crystal. One is bound in the active site opposite the sulfonamide group of **17** and forms contacts to the side chain hydroxyl groups of Ser87 and Ser118 and the backbone carbonyl of Met120, clearly identifying new solvent exposed target sites on the protein.

Structures for the related compounds **79** and **85** (Figure 2B, C) were also determined, and the binding modes were in good agreement with that of **17**; the structure data are presented in Table S2. The carboxylate-containing **85** showed good overlap with the benzoic acid, sulfonyl, and 6,6 cyclic systems of **17**, although the napthyl and tetrahydroquinoline groups do have alternative orientations. This structure also showed an acetate bound to the ethylene glycol binding site described above, forming a hydrogen bond with the Ser82 side chain hydroxyl

Scheme 3. Compounds of Table 6[a]
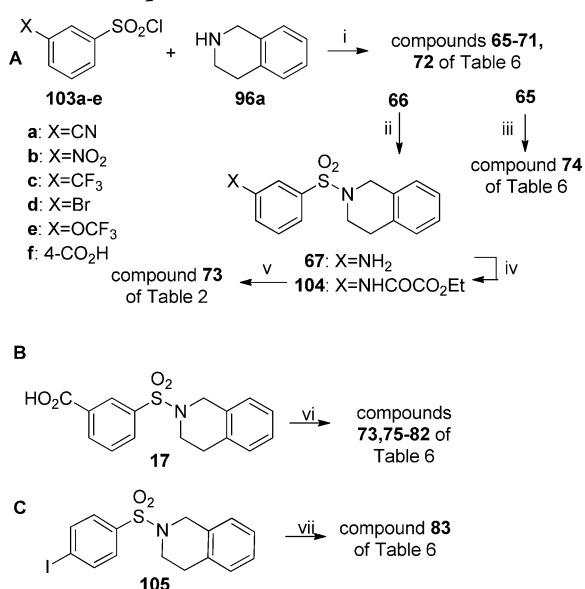
[a]Reagents: (i) K_2CO_3 or Et_3N, pyridine, dioxan or Me_2CO, 20 °C, 2–90 h; (ii) Fe, AcOH, DMF, EtOH, H_2O, reflux, 1 h; (iii) NaN_3, NH_4Cl, DMF, 120 °C, 69 h; (iv) $ClCOCO_2Et$, pyridine, THF, 10–20 °C, 1 h; (v) Cs_2CO_3, THF, H_2O; (vi) **17**, $(COCl)_2$, CH_2Cl_2, DMF (cat.) or CDI, THF, then RNH_2, 20 °C, 1–4 h; (vii) 2-pyrrolidinone, Pd_2dba_3, Xantphos, Cs_2CO_3, dioxane, 100 °C, 18 h.

Scheme 4. Compounds of Table 7[a]
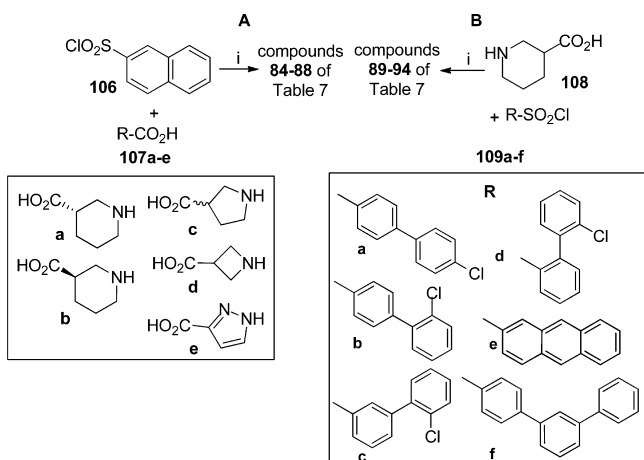
[a]Reagents and conditions: (i) Et_3N or K_2CO_3, Me_2CO or THF, N_2, 0–20 °C, 3–90 h.

group (Figure 2C). The structure of **79** bound showed that the amide carbonyl group of the methylbenzamide analogue **79** was within hydrogen bond distance of His117 and Tyr55 (Figure 2B). To accommodate the carboxamide, the carbonyl group has rotated away from the oxyanion hole, displacing the benzyl group relative to that of **17**, causing the sulfonamide to move further into the active site pocket and the position occupied by an ethylene glycol, and acetate molecule in **17** and **85**, respectively, is now occupied by a water molecule.

When compared to other carboxylate-containing NSAIDs with known binding modes, including flufenamic acid (**11**), the binding mode of **17** most closely resembled that of **11** (Figure 2D, E). There is good agreement between the benzoic acid moieties of both compounds, while the aniline unit of **11**

transitions through the same space as the sulfonamide group in **17**, positioning, the CF_3 group in close proximity to the piperidine ring of the tetrahydroquinoline in **17**. While it is likely that the increased potency of **17** is related to the better occupation of an active site pocket by the tetrahydroquinoline, its complementarity with the active site may also be aided by the rigid "butterfly" shape formed by the sulfonamide. Moreover, the small difference in activity between 17 and 79 indicates that occupation of the oxyanion hole by a carboxylate group has a minor but detectable role in inhibition.

To gain some insight into the complementary between the rigid "butterfly" shape of the embedded sulfonamide linker and the AKR1C3 active site, we compared energy and conformational differences for ligands minimized in and out of the AKR1C3 active site (Table 4). Ligands were initially minimized within the active site and for the sulfonamide compounds **17** and **79**, as well as the N-phenylanthranilic acid flufenamic acid (**11**); the rmsd of the respective minimized conformation was within 0.26, 0.43, and 0.33 Å of the initial structure respectively, while the minimized conformation of **85** showed greater deviation at 0.67 Å. These ligand conformations were then minimized without the active site constraint, and the lower energy difference between the bound and free minimized conformations implied that the sulphonamides **17** and **79** are less strained in the active site than flufenamic acid (**11**). This was also to some extent supported by the lower rmsd values, with **17** and **79** having the lowest deviation from the minimized active site geometry while flufenamic acid (**11**) had the highest. The low differences in strain between the bound and unbound forms indicate that **17** and **79** are likely more rigid and better adapted to the AKR1C3 active site than flufenamic acid (**11**); this is also evident in the calculated ligand–protein interaction energy (LPE) and may in part account for the difference in potency.

■ STRUCTURE ACTIVITY RELATIONSHIPS

The AKR1C3 preference for the tetrahydroquinoline system of **17** was investigated with compounds **18–23** in Table 2 and with **56–64** in Table 5. The data in Table 2 shows that altering the size or orientation of the tetrahydroquinoline piperidine group, while retaining AKR1C3 inhibitory activity, decreases the potency from 2- to 46-fold compared to **17**. Comparison of the data for **17** and the tetrahydroquinoline isostere **19**, when compared to that of **20–22**, clearly shows that the potency of **17** depends on the orientation of tetrahydroquinoline group. The 46-fold reduction in IC_{50} of **23** compared to **17** also indicates the importance of the ring-embedded sulfonamide linker.

A series of open chain analogues presented in Table 5 provided a more divergent set of sulfonamide probes that explore the active site's capacity to bind different structures. These substantially more flexible compounds were weaker inhibitors than **17**. Thus, compound **56**, the direct open-chain analogue of **17**, was 17-fold less potent, and the set of compounds were on average 28-fold less potent than **17** against AKR1C3. Overall, these data clearly support the preference of the AKR1C3 active site for a rigid bicyclic system.

Analogue sets around the tetrahydroquinoline core of **17** were developed to probe the interaction with the buried part of the active site, and the results are presented in Table 3. Based on the binding mode of **17**, substitutions around the 5-position may better fill part of the active site defined by the side chains of Met120, Pro318, Asn167, Tyr319, and Tyr216 and three
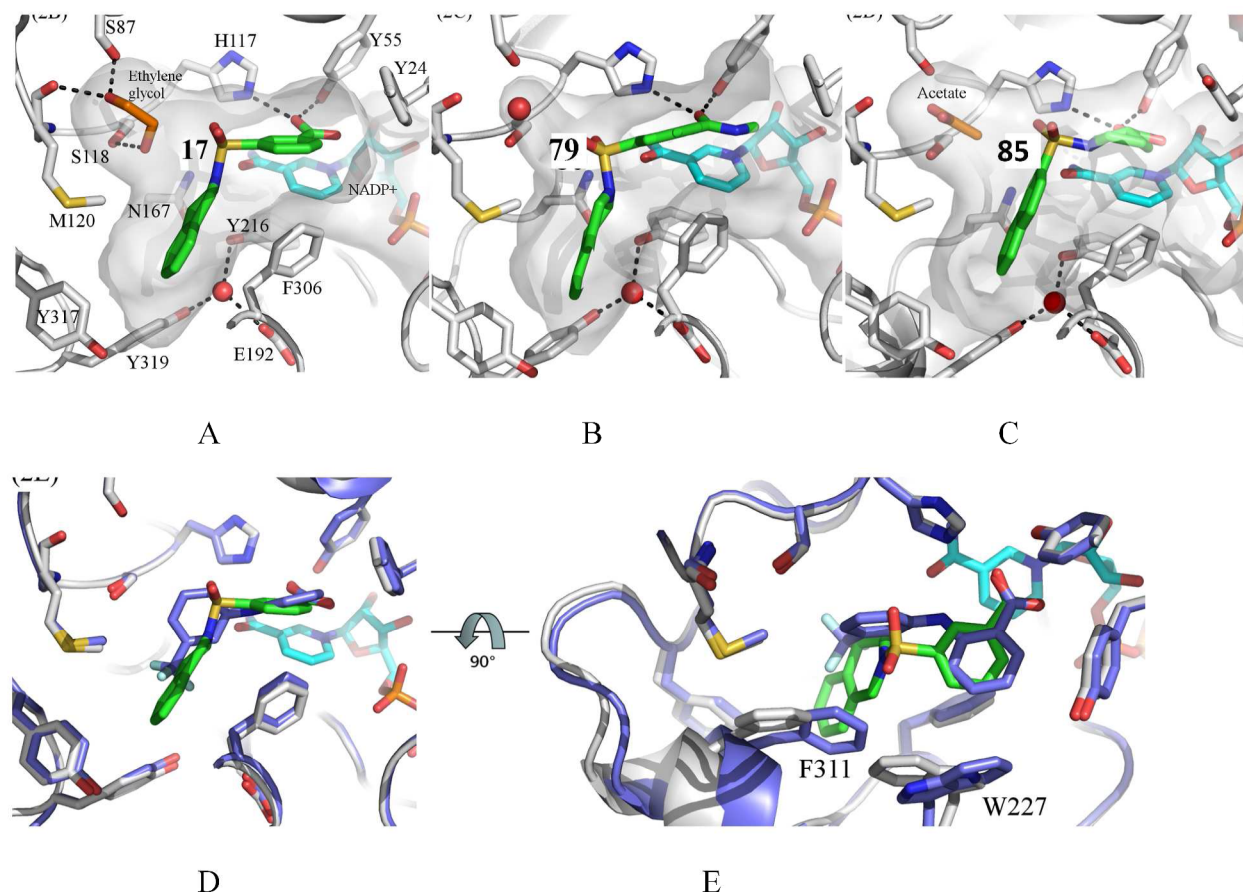
Figure 2. X-ray structures for AKR1C3 in complex with compounds **17** (2A), **79** (2B), and **85** (2C). Carbon atoms for the protein, compound, and NADP$^+$ are colored gray, green, and cyan, respectively. Key hydrogen bonds are represented as dotted lines. The surface of the active site cavity is shown in gray with residues defining the pocket labeled. The water molecule located in a pocket formed by the side chains of Y216, Y319, and E192 is represented as a red sphere. An ethylene glycol molecule carried over from crystal freezing is bound in the active site of the structure with compound **17**, whereas an acetate molecule carried over from the crystallization condition occupies an equivalent position in the structure with compound **85** (2D and 2E). Comparison between the structures of AKR1C3 in complex with compound **17** (green carbon atoms) and compound **11** (flufenamic acid; PDB code = 1S2C; purple carbon atoms) viewed from the side (2D) and above the plane of the nicotinamide ring of the NADP$^+$ (2E). Differences in binding modes cause a shift in position of the side chains of F311 and W227. Figure prepared using PyMOL (The PyMOL Molecular Graphics System, Version 1.3, Schrödinger, LLC).

Table 4. Comparison of Strain Energies for the Bound and Unbound Ligands

compd	$E_{[Bound]}$	$E_{[Free]}$	ΔE	rmsd	LPE
11	−7.46	−14.75	7.29	0.62	−9.87
17	−75.60	−77.29	1.69	0.16	−20.90
79	−32.98	−35.91	2.93	0.23	−16.87
85	−99.61	−106.25	6.64	0.32	−4.15

ordered water molecules not accessed by the tetrahydroquinoline core. Consistent with this, substitutions that introduced hydrogen bond donor and acceptor groups or lipophilic moieties were well tolerated. Similarly, substitutions at the 6-position were also well tolerated. By contrast, informed by the experimentally derived binding mode, substitutions at the 7-position were expected to be less tolerated, as this position is 4.04 Å of the backbone amide unit of Asn302. As seen in Table 3, a range of simple substituents at the 6-position appear to be very well tolerated, with many compounds having AKR1C3 IC$_{50}$ values comparable to (and up to 2-fold superior; **38**) that of the parent **17**. Several of these also demonstrate improved selectivity relative to AKR1C1. However, there are limits to the size of this binding pocket; while the acetylene **43** is only 3-fold

Table 5. SAR for Analogous "Open-Chain" 3-(*N*-Phenethylsulfamoyl)benzoic Acids

		IC$_{50}$ $(\mu M)^{a,b}$				
no.	R	1C1	1C2	1C3	1C4	HCT-116[b]
56	H	>30	>30	0.22 ± 0.16	>30	>1
57	2-F	>30	>30	0.33 ± 0.13	>30	
58	3-Cl	>30	>30	0.21 ± 0.05	>30	>1
59	4-Cl	>30	>30	0.14 ± 0.08	>30	>1
60	3-OMe	>30	>30	0.74 ± 0.29	>30	
61	4-OMe	>30	>30	1.44 ± 0.11	>30	
62	3-OPh	>30	>30	0.53 ± 0.21	>30	
63	3-Me	>30	>30	0.22 ± 0.05	>30	
64	4-Me	>30	>30	0.64 ± 0.07	>30	

[a,b]As for Table 2.

less potent that **17**, the much larger 4-trifluoromethoxyphenylacetylene **44** is 100-fold less potent. Overall, the most potent compound was the 6-bromo analogue **38**, with about 5000-fold

selectivity for AKR1C3 over the other three isoforms. Superposition of all human AKR1C3 entries in the PDB indicated that the loop structure adjacent to position 7 can undergo some conformational change and may be enough to accommodate some substitutions.

The function of the carboxylate in ligand binding was examined with the compounds presented in Table 6. This

Table 6. SAR for Ring A Substituents for Inhibition of AKR Isoforms
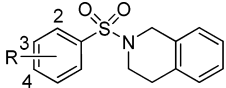
No	R	IC$_{50}$ (μM)[a]				
		1C1	1C2	1C3	1C4	HCT-116[b]
65	3-CN			>30		
66	3-NO$_2$			>30		
67	3-NH$_2$			>30		
68	3-CF$_3$			>30		
69	3-Br			>30		
70	3-OCF$_3$			>30		
71	4-CO$_2$H	>30	>30	1.24±0.42	>30	>1
72	3-NHCOCO$_2$H	>30	>30	0.062±0.011	>30	>1
73	3-CONHSO$_2$NH$_2$			>30		
74	3-tetrazole	>30	>30	0.0095±0.0078	>30	0.897
75	3-CONH$_2$	>30	>30	0.17±0.09	>30	
76	3-CONHmorpholide	>30	>30	0.078±0.02	>30	0.013
77	3-CONHthiomorpholide	>30	>30	0.45±0.09	>30	
78	3-CONH(CH$_2$)$_2$NMe$_2$	>30	>30	0.90±0.40	>30	
79	3-CONHMe	>30	>30	0.050±0.016	>30	0.013±0.001
80	3-CONMe$_2$	>30	>30	0.053±0.024	>30	0.014
81	3-CO-N◇O	>30	>30	0.35±0.04	>30	
82	3-CONH(CH$_2$)$_2$(4-pyridyl)	>30	>30	0.058±0.006	>30	0.035
83	4-(pyrrolidinone)	>30	>30	0.042±0.021	>30	0.024

[a,b]As for Table 2.

showed that both the nature and positioning of the acid group were critical. A variety of other 3-substituents, including H-bond donor groups such as amino, were completely ineffective (compounds 65−70), and even positioning the acid group at the neighboring 4-position gave a compound (71) nearly 100-fold less potent than 17. However, compounds 72 and 74 showed that acid isosteres were acceptable as H-bond acceptors at the 3-position.

Inspection of the structure of 17 indicated that substituents around the phenyl ring may occupy an extended cavity distal to the oxyanion hole that has one wall defined by the cofactor NADPH, and a small series of 3-amides of varying size, pK$_a$, and rigidity (75−82) were made to explore this. These

compounds exhibited slightly reduced potency compared to acid 17 but still had IC$_{50}$ values in the submicromolar range. Both simple secondary (79) and tertiary (80) amides were acceptable, as was a range of analogues bearing solubilizing units. The least effective of these was the strong base 78, which was 70-fold less effective than 17. Strikingly, the 4-pyrrolidinone 83 was only 3-fold less potent than the parent compound, 17, with an IC$_{50}$ of 0.042 μM. It is also noteworthy that 3-(4-pyridinyl)ethyl amide 82 is also reasonably active, being only 4-fold less potent than 17. This tolerance of the extended aromatic substitution of 82 suggests some flexibility inherent to the cavity about the A-ring.

Finally, Table 7 shows a set of "reverse sulfonamides". Compounds 84−88 have the carboxylic acid attached to a set

Table 7. SAR for "Reverse" Sulfonamides

No	R	IC$_{50}$ (μM)[a]				
		1C1	1C2	1C3	1C4	HCT-116[b]
84		>30	>3[c]	0.40±0.08	>3[c]	>1
85		>30	>30	0.032±0.023	>30	>1
86		22.2±0.5	>30	0.38±0.057	>30	
87				>30		
88		15.0±1.1	>30	0.50±0.27	>30	
89				>30		
90		11.0±1.4	>30	0.55±0.15	>30	
91		>30	>30	0.74±0.15	>30	
92				>30		
93		>30	>30	0.39±0.20	>30	
94		0.73±0.34	>30	24.4	>30	
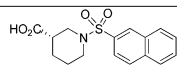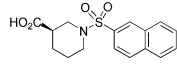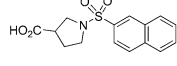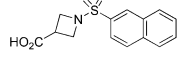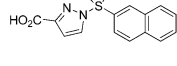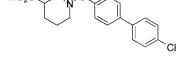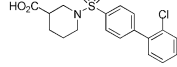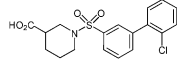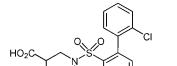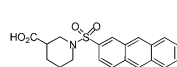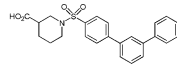
[a,b]As for Table 2. [c]84 showed <10% inhibition at 3 μM.

of alicyclic and aromatic heterocycles that position it differently. Compound 85 is of particular interest as a potent inhibitor of AKR1C3. Determination of the crystal structure of its complex with the enzyme showed that alternative ring systems could appropriately present the carboxylate group to the oxyanion hole. The IC$_{50}$ data for compounds 84 and 85 showed the S stereoisomer was about 12-fold less active (IC$_{50}$s 0.40 and 0.032 μM, respectively). The pyrrolidone 86 and pyrazole 88 analogs had similar potency to 84, while the azetidine 87 was

inactive. Compounds **89−94** retain the (racemic) piperidine carboxylic acid and explore an alternative for the bicyclic unit. Compounds **90**, **91**, and **93** retain some activity, but those (**89**, **92**, **94**) with more bulky units were inactive, demonstrating again the limits of the lipophilic binding pocket.

While the vast majority of the compounds showed no discernible activity (IC$_{50}$ > 30 μM) against the other three AKR1 isoforms, there were a few exceptions, from which some SAR can be discerned. Compound **24**, one of three compounds with substantial activity (IC$_{50}$ < 1 μM) against AKR1C1, is also the only compound in the set with an additional fused aromatic ring on the acid-bearing unit. Of the only other compounds with AKR1C1 IC$_{50}$s < 1 μM, **53** is the only 8-substituted analogue and **94** has the most extended amine-bearing unit. Compound **94** also has 33-fold selectivity for AKR1C3 over the other three isoforms, which may reflect differences in the shape/size of the hydrophobic pocket. The only compound among the NSAIDs of Table 1 or the {dihydroisoquinolin-2[1*H*]-yl}sulfonyl)benzoic acids studied here with an IC$_{50}$ < 10 μM against AKR1C4 was the 7-tetrazole **45**. This, taken together with the relative loss of AKR1C3 activity for compound **44**, which bears a very bulky 7-substituent, suggests that exploration of further (hetero)aromatic systems at this position might yield selective AKR1C4 analogues. Finally, the 5-chloro (**29**) and 8-chloro (**53**) analogues were the only compounds to show any activity against AKR1C2; while this was only weak (IC$_{50}$ 9.3 and 12.1 μM, respectively), it was unexpected.

CELLULAR ACTIVITY

Selected compounds displaying the greatest potency against the isolated AKR1C3 isoenzyme were also evaluated for their effectiveness in human HCT-116 colon cancer cells engineered to overexpress AKR1C3. The assay utilized an exogenous dinitrobenzamide substrate, PR-104A (see Supporting Information for structure), which is exclusively metabolized by AKR1C3 under aerobic conditions to its cytotoxic 4-hydroxyl-amine (PR-104H) and 4-amine (PR-104M) metabolites.[6] The effectiveness of compounds at inhibiting AKR1C3 activity in these cells was measured by their ability to inhibit this metabolism. The parent compound **17** was able to inhibit AKR1C3 activity (inhibiting PR-104H formation) with an IC$_{50}$ of 0.027 ± 0.002 μM. For the majority of the 45 compounds evaluated in the HCT-116 assay, there was a broad rank order between enzymatic and cellular activity, with some exceptions. Compounds showing significantly less activity in the cellular assay than expected by the above ranking were the more polar ones (the OH- and NO$_2$-substituted acids **32** and **35** and the tetrazole isostere **74**), and the aminooxoacetic acid **72**, which may be due to poorer uptake. This is reinforced by the fact that most of the neutral amides in Table 6 (e.g., **76**, **79**, **80**, **83**) showed better than expected cellular activity. Three other compounds whose poorer cellular activity could not be explained on pharmacological grounds did have unique structures: the only 2-substituted dihydroisoquinoline **26** and the two angular-substituted analogues **20** and **22**.

CONCLUSIONS

The results show that the 3-(3,4-dihydroisoquinolin-2(1*H*)-ylsulfonyl)benzoic acids are novel, very potent, and highly isoform-selective inhibitors of the AKR1C3 enzyme (up to an IC$_{50}$ of 6.1 nM for AKR1C3 with approximately 5,000-fold

selectivity over the other three isoforms for compound **38**). The broad requirement for an acid, isostere, or amide at the 3-position is consistent with the crystal structure data (interaction with Tyr55 and His117 at the oxyanion hole site). The 30-fold loss in potency in going from **17** to **18** (loss of the benzene ring) shows that the dihydroisoquinoline makes important hydrophobic interactions in a cavity defined by residues Asn167, Tyr216, Phe306, Tyr319, and Tyr317 (Figure 2B). A wide variety of small substituents on the benzene were tolerated, including the 7-alkyne **43**, but the corresponding 2-(4-methoxyphenyl)alkyne **44** was 100-fold less potent, suggesting limits to this cavity. The compounds also showed good potency in a cellular assay, blocking the ability of AKR1C3 to metabolize a proven substrate. The high potency and selectivity of the class for AKR1C3 over both other AKR1C isoforms and over COX1 and COX2 make them of considerable interest as both therapeutic inhibitors and biological tools.

EXPERIMENTAL SECTION

Combustion analyses were performed by the Campbell Micro-analytical Laboratory, University of Otago, Dunedin, New Zealand. Melting points were determined on an Electrothermal IA9100 melting point apparatus and are as read. NMR spectra were measured on a Bruker Avance 400 spectrometer at 400 MHz for ^{1}H and are referenced to Me$_4$Si. Chemical shifts and coupling constants are recorded in units of parts per million and hertz, respectively. High-resolution electron impact (HREIMS) and fast atom bombardment (HRFABMS) mass spectra were determined on a VG-70SE mass spectrometer at nominal 5000 resolution. High-resolution electrospray ionization (HRESIMS) and atmospheric pressure chemical ionization (HRAPCIMS) mass spectra were determined on a Bruker micrOTOF-Q II mass spectrometer. Low-resolution atmospheric pressure chemical ionization (APCI) mass spectra were measured for organic solutions on a ThermoFinnigan Surveyor MSQ mass spectrometer, connected to a Gilson autosampler. Thin-layer chromatography was carried out on aluminum-backed silica gel plates (Merck 60 F$_{254}$), with exposure to I$_2$, or by staining in permanganate and phosphomolybdic acid dips and by UV light (254 and 365 nm). Column chromatography was carried out on silica gel (Merck 230−400 mesh). Compounds of Tables 1 and 2 were isolated following trituration in Et$_2$O, unless otherwise indicated. Tested compounds were ≥95% pure, as determined by combustion analysis, or by HPLC conducted on an Agilent 1100 system, using a reversed phase C8 column with diode array detection.

Chemistry: General Procedures. *Method A.*[22] A solution/suspension of the amine or amine hydrochloride salt (1.00 or greater equiv) in acetone or THF (∼0.03−0.30 M, AR grade) under N$_2$ was treated with Et$_3$N or K$_2$CO$_3$ (1.0 equiv, or greater, especially if amine was an HCl salt) and DMF (∼0.50−3.50 M, dry), and the resulting mixture was cooled to 0 °C in an ice−water bath. A solution of the sulfonyl chloride (1 equiv) in acetone (∼0.03−0.30 M, AR grade) was then slowly added dropwise, and the resulting mixture was allowed to warm to 20 °C over 3−90 h. After analysis (TLC, APCI) showed the reaction was complete, the reaction mixture was filtered through a Celite pad, and the solvent was removed under reduced pressure. The residue was extracted into 1 M NaOH, and the resulting suspension was filtered through a Celite pad. The filtrate was acidified with dilute HCl (1 M) to afford a suspension, filtration of which afforded solid crude product. (Alternatively, the residue was resuspended in EtOAc and extracted with 1 M NaOH. The aqueous layer was filtered and then acidified with 1 M HCl, and the resulting suspension was filtered to give a solid.) Reprecipitation of this solid from an appropriate solvent system, and/or purification by column chromatography on silica gel, furnished the desired sulfonamide.

Method B.[27] Methanesulfonic acid (0.4 mL per mmol of sulfonamide) and *s*-trioxan (0.3 equiv) were added to a solution/

suspension of sulfonamide (1.00 equiv) in 1,2-dichloroethane (~0.2 M) under N_2, and the resulting solution/suspension was stirred at 35 °C overnight. After analysis (TLC, APCI) showed the reaction was complete, the reaction mixture was cooled to 20 °C and then filtered. The collected solid was purified by reprecipitation from EtOAc/hexanes, with further purification by column chromatography on silica gel, if necessary, to afford the product sulfonamide.

Compounds of Table 2 (Scheme 1A). *3-({5,6-Dihydropyridin-1[2H]-yl}sulfonyl)benzoic Acid (18).* Reaction of 3-(chlorosulfonyl)-benzoic acid (**95**) and 1,2,3,6-tetrahydropyridine by method A, followed by recrystallization of the crude product from EtOAc/hexanes, afforded **18** (58%, unoptimized) as cream flaky crystals; mp 166−168 °C; ^{1}H NMR [(CD$_3$)$_2$SO]: δ 13.54 (br s, 1H), 8.23 (m, 2H), 8.01 (dt, J = 7.9, 1.5 Hz, 1H), 7.78 (m, 1H), 5.73 (m, 1H), 5.65 (m, 1H), 3.53 (m, 2H), 3.14 (t, J = 5.7 Hz, 2H), 2.12 (m, 2H); HRESIMS calcd for C$_{12}$H$_{14}$NO$_4$S m/z [M + H]$^+$ 268.0638, found 268.0641; HPLC purity 98.9%.

See Supporting Information for details of the syntheses of related compounds **19−23** of Table 2 from sulfonic acid **95**.

Compounds of Table 3 (Scheme 1B, C). *3-({3,4-Dihydroiso-quinolin-2[1H]-yl}sulfonyl)benzoic Acid (17).*[21] Reaction of 3-(chlorosulfonyl)benzoic acid (**95**) and 1,2,3,4-tetrahydroisoquinoline (**96a**) by method A, followed by reprecipitation of the crude product from EtOAc/hexanes, afforded **17** (yield 50%, unoptimized) as an amorphous white solid; mp 276−280 °C; ^{1}H NMR [(CD$_3$)$_2$SO]: δ 13.53 (br s, 1H), 8.27 (t, J = 1.6 Hz, 1H), 8.21 (d, J = 7.8 Hz, 1H), 8.07 (dt, J = 7.8, 1.5 Hz, 1H), 7.76 (t, J = 7.8 Hz, 1H), 7.13 (m, 4H), 4.24 (s, 2H), 3.35 (t$_{overlap\ water\ peak}$, J = 6.0 Hz, 2H), 2.84 (t, J = 6.0 Hz, 2H); HRESIMS calcd for C$_{16}$H$_{15}$NO$_4$S m/z [M + H]$^+$ 318.0795, found 318.0794; HPLC purity 99.8%.

See Supporting Information for details of the syntheses of related compounds **25−33, 35, 36, 38−41, 46, 47,** and **49−50** of Table 3 from sulfonic acid **95**.

3-({6-Chloro-3,4-dihydroisoquinolin-2[1H]-yl}sulfonyl)benzoic Acid (37). Reaction of sulfonamide **63** with methanesulfonic acid and s-trioxan by method B, followed by reprecipitation of the crude product from EtOAc/hexanes, and then column chromatography on silica gel (eluting with 0−40% EtOAc/hexanes + 0.5% v/v CH$_3$CO$_2$H), afforded **37** (35%, unoptimized) as an amorphous white solid; mp 202−203 °C; ^{1}H NMR [(CD$_3$)$_2$SO]: δ 13.51 (br s, 1H), 8.27 (t, J = 1.6 Hz, 1H), 8.21 (dt, J = 7.8, 1.3 Hz, 1H), 8.06 (d, J = 8.2 Hz, 1H), 7.76 (t, J = 7.8 Hz, 1H), 7.21 (m, 3H), 4.25 (s, 2H), 3.35 (t$_{overlap\ water\ peak}$, J = 6.0 Hz, 2H), 2.84 (t, J = 6.0 Hz, 2H); HRESIMS calcd for C$_{16}$H$_{15}$Cl NO$_4$S m/z [M + H]$^+$ 354.0376, 352.0405, found 354.0385, 352.0407; HPLC purity 97.1%.

See Supporting Information for details of the syntheses of related compounds **34, 42,** and **48** of Table 3 from compounds **58, 64,** and **59**, respectively, of Table 5.

3-((7-Ethynyl-3,4-dihydroisoquinolin-2(1H)-yl)sulfonyl)benzoic Acid (43). A solution of iodide **50** (0.43 g, 0.96 mmol, 1.00 equiv) in CH$_3$CN (10 mL) and DMF (15 mL) was treated sequentially with Pd(PPh$_3$)$_4$ (60 mg, 0.05 mmol, 0.05 equiv), CuI (11 mg, 0.06 mmol, 0.06 equiv), (trimethylsilyl)acetylene (**97**) (0.23 mL, 1.63 mmol, 1.70 equiv) and *N,N*-diisopropyl ethylamine (0.28 mL, 1.63 g, 1.70 equiv).[28,29] The resulting mixture was deoxygenated by five N$_2$-flush−evacuate cycles and then stirred at 20 °C for 48 h. The reaction mixture was then diluted with water and saturated aqueous NH$_4$Cl and then extracted with CH$_2$Cl$_2$ (×4). The combined organic layers were washed with brine, dried (MgSO$_4$), and evaporated under reduced pressure. The resulting crude products from two equal runs were combined and chromatographed on silica gel, eluting with 0−50% EtOAc/hexanes + 0.5% v/v AcOH to afford 3-((7-((trimethylsilyl)-ethynyl)-3,4-dihydroisoquinolin-2(1*H*)-yl)sulfonyl)benzoic acid (**98**) (0.27 g, 37% combined yield) as an amorphous off-white solid (APCI−): m/z 413.1; TLC R_f 0.47 (50% EtOAc/hexanes + 3 drops AcOH)), which was used without further purification.

A solution of the TMS ethyne **98** (78 mg, 0.19 mmol, 1.00 equiv) in MeOH (4 mL) was treated with anhydrous Cs$_2$CO$_3$ (0.19 g, 0.59 mmol, 3.12 equiv), and the resulting dark brown solution was stirred at 20 °C for 100 min and then diluted with saturated aqueous NH$_4$Cl

and extracted with EtOAc (×4).[28,30] The combined organic extracts were washed with brine, dried (MgSO$_4$), and evaporated under reduced pressure to afford crude product. This was combined with a second run from 161 mg of **98** and by chromatography on silica gel, eluting with 0−50% EtOAc/hexanes + 0.5% v/v AcOH followed by reprecipitation from EtOAc/hexanes, to yield **43** (21 mg, 11%, unoptimized) as an amorphous pale pink solid: mp 224−227 °C; ^{1}H NMR [(CD$_3$)$_2$SO]: δ 13.54 (v br s, 1H), 8.27 (t, J = 1.6 Hz, 1H), 8.21 (dt, J = 7.8, 1.3 Hz, 1H), 8.06 (d, J = 8.0 Hz, 1H), 7.76 (t, J = 7.8 Hz, 1H), 7.32 (s, 1H), 7.23 (dd, J = 7.9, 1.5 Hz, 1H), 7.11 (d, J = 8.0 Hz, 1H), 4.25 (s, 2H), 4.11 (s, 1H), 3.35 (t, J = 6.0 Hz, 2H), 2.84 (t, J = 5.9 Hz, 2H); HRESIMS calcd for C$_{18}$H$_{16}$NO$_4$S m/z [M + H]$^+$ 342.0795, found 342.0792; HPLC purity 96.7%.

3-((7-((4-(Trifluoromethoxy)phenyl)ethynyl)-3,4-dihydroisoquino-lin-2(1H)-yl)sulfonyl)benzoic Acid (44). Based on the procedures described by Gu et al.,[31] 1-ethynyl-4-(trifluoromethoxy)benzene (**99**) (0.035 mL, 0.23 mmol, 1.00 equiv) was added to a mixture of iodide **50** (100 mg, 0.23 mmol, 1.00 equiv) and Pd(PPh$_3$)$_2$Cl$_2$ (6 mg, 0.009 mmol, 0.04 equiv) in piperidine (1.00 mL, 2.26 mmol, 45 equiv) at 20 °C. The resulting semisolid yellow-white mixture was heated to 85 °C to form an orange solution and was then stirred at this temperature for a further 12 h. The reaction mixture was cooled to 20 °C, diluted with H$_2$O and 15% HCl, and then extracted with Et$_2$O (×4). The combined organic layers were washed with water until neutral and then dried (MgSO$_4$) and concentrated to dryness under reduced pressure. The residue was reprecipitated from EtOAc/hexanes to furnish **44** (21 mg, 20%, unoptimized) as an amorphous off-white solid; mp 235−238 °C; ^{1}H NMR [(CD$_3$)$_2$SO]: δ 13.62 (v br s, 1H), 8.28 (t, J = 1.6 Hz, 1H), 8.21 (dt, J = 7.8, 1.4 Hz, 1H), 8.05 (d, J = 8.0 Hz, 1H), 7.75 (t, J = 7.8 Hz, 1H), 7.66 (ddd, J = 9.4, 4.8, 2.7 Hz, 2H), 7.42 (m, 3H), 7.33 (dd, J = 7.9, 1.5 Hz, 1H), 7.16 (d, J = 8.0 Hz, 1H), 4.29 (s, 2H), 3.38 (t, J = 6.0 Hz, 2H), 2.87 (t, J = 5.8 Hz, 2H); HRESIMS calcd for C$_{25}$H$_{18}$F$_3$NO$_5$S m/z [M + H]$^+$ 502.0931, found 502.0940; HPLC purity 98.7%.

3-((7-(2H-Tetrazol-5-yl)-3,4-dihydroisoquinolin-2(1H)-yl)-sulfonyl)benzoic Acid (45). Following the method of Nakamura et al.,[32] sodium azide (102 mg, 1.57 mmol, 1.25 equiv) was added to a mixture of nitrile **51** (430 mg, 1.27 mmol, 1.00 equiv) and NH$_4$Cl (84 mg, 1.57 mmol, 1.25 equiv) in DMF, and the resulting mixture was stirred at 120 °C for 171 h. After this time, the reaction mixture was cooled to 20 °C and then concentrated to dryness under reduced pressure. Trituration of the resulting brown gum in an ultrasonic bath afforded a glutinous tan solid, which was reprecipitated from MeOH/EtOAc/hexanes to furnish **45** (327 mg, 68%) as an amorphous white solid; mp: 246 °C (dec.); ^{1}H NMR [(CD$_3$)$_2$SO]: δ 14.77 (br s, 1H), 8.28 (t, J = 1.6 Hz, 1H), 8.21 (dt, J = 7.9, 1.3 Hz, 1H), 8.09 (dd, J = 7.9, 1.8, 1.2 Hz, 1H), 7.86 (s, 1H), 7.77 (m, 2H), 7.31 (d, J = 8.0 Hz, 1H), 4.37 (s, 2H), 3.41 (t, J = 6.0 Hz, 2H), 2.91 (t, J = 6.0 Hz, 2H) {tetrazole -NH- not visible}; HRESIMS calcd for C$_{17}$H$_{15}$N$_5$NaSO$_4$Cl m/z [M + Na]$^+$ 408.0737, found 408.0748; HPLC purity 96.9%.

5-((3,4-Dihydroisoquinolin-2(1H)-yl)sulfonyl)nicotinic Acid (55). 2,4-Dichloro-5,5-dimethylhydantoin (2.42 g, 12.27 mmol, 1.61 equiv) was added portionwise to a solution of methyl 5-mercaptonicotinate[23] (**100**) in MeCN/AcOH/water (40:1.5:1.0, 128 mL) cooled at 0 °C such that the reaction temperature remained <10 °C. Once the addition was complete, the reaction mixture was allowed to warm to and stirred at 20 °C for 110 min; then almost all solvent was removed under reduced pressure (<30 °C), and the resulting concentrated solution was diluted with CH$_2$Cl$_2$ (8 mL) and cooled to 0 °C. This solution was treated with 5% NaHCO$_3$ (53 mL), at such a rate that the temperature remained <10 °C. The resulting mixture was stirred at 0−5 °C for 15 min and then separated. The organic layer was washed with a cooled (<10 °C) solution of 10% brine and then dried (MgSO$_4$) and filtered. Solvent was removed under reduced pressure (bath temperature 30 °C) to afforded methyl 5-(chlorosulfonyl)-nicotinate (**101**) as a yellow viscous oil (1.18 g), which was used without further purification, as soon as possible.

101 (0.066 g, 0.28 mmol, 1.00 equiv) was reacted with 1,2,3,4-tetrahydroisoquinoline (**96a**) (0.42 mL, 0.34 mmol, 1.20 equiv) by method A, and the resulting crude ester (39 mg, 0.12 mmol, 1.00

equiv) was dissolved in MeOH (5.8 mL) and water (3.9 mL) and treated with anhydrous LiOH (9 mg, 0.40 mmol, 3.38 equiv) with stirring at 20 °C for 80 min, when all starting material was consumed (TLC). Solvent was removed under reduced pressure, the residue was redissolved in H_2O (50 mL) and acidified to pH 1 by addition of 1 M HCl (~1 mL), and the product was collected by filtration, washed with hexanes, and dried to afford crude **55** as an amorphous pale yellow solid. The product from two reactions was combined and reprecipitated from EtOAc/hexanes to give pure **55** (87 mg, 30%) as an amorphous tan solid; mp 233–237 °C; ^{1}H NMR [(CD$_3$)$_2$SO]: δ 14.06 (br s, 1H), 9.26 (d, J = 1.9 Hz, 1H), 9.17 (d, J = 2.2 Hz, 1H), 8.48 (d, J = 2.1 Hz, 1H), 7.22–7.05 (m, 4H), 4.33 (s, 2H), 3.44 (t$_{overlap\ water\ peak}$, J = 6.0 Hz, 2H), 2.84 (t, J = 6.0 Hz, 2H); HRESIMS calcd for $C_{15}H_{15}N_2O_4S$ m/z (M + H)$^+$ 319.0747, found 319.0747; HPLC purity 98.6%.

Compounds of Table 5 (Scheme 2). 3-(N-Phenethylsulfamoyl)-benzoic Acid (56). Reaction of 3-(chlorosulfonyl)benzoic acid (**95**) and 2-phenylethanamine (**102a**) (5.00 equiv), under the conditions used to prepare acid **49**, gave **56** (53%) as an amorphous white solid; mp 188–190 °C; ^{1}H NMR [(CD$_3$)$_2$SO]: δ = 13.44 (br s, 1H), 8.31 (t, J = 1.6 Hz, 1H), 8.16 (d, J = 7.8 Hz, 1H), 7.99 (d, J = 8.1 Hz, 1H), 7.85 (t, J = 5.7 Hz, 1H), 7.71 (dd, J = 7.8, 7.7 Hz, 1H), 7.25 (m, 2H), 7.18 (m, 1H), 7.14 (m, 2H), 2.99 (m, 2H), 2.81 (dd, J = 7.6, 7.2 Hz, 2H); HRESIMS calcd for $C_{15}H_{15}NNaO_4S$ m/z [M + Na]$^+$ 328.0614, found 328.0610; TLC; HPLC purity 98.8%.

See Supporting Information for details of the syntheses of related compounds **57–64** of Table 5 from sulfonyl chloride **95** and amines **102b–h**.

Compounds of Table 6 (Scheme 3A). 3-((3,4-Dihydroisoqui-nolin-2(1H)-yl)sulfonyl)benzonitrile (65). A suspension of 1,2,3,4-tetrahydroisoquinoline (**96a**) (0.76 g, 6.05 mmol, 1.00 equiv) and 3-cyanobenzene-1-sulfonyl chloride (**103a**) (1.22 g, 6.05 mmol, 1.00 equiv) in acetone (17 mL) was treated with Et$_3$N (0.84 mL, 6.05 mmol, 1.00 equiv), and the resulting viscous suspension was stirred vigorously for 3 days at 20 °C. The mixture was then filtered, and the crude product was collected and reprecipitated to give **65** (247 mg, 14%, unoptimized) as an amorphous white solid; mp 192–194 °C; ^{1}H NMR [(CD$_3$)$_2$SO]: δ 8.25 (t, J = 1.6 Hz, 1H), 8.14 (m, 2H), 7.81 (t, J = 7.9 Hz, 1H), 7.21–7.12 (m, 3H), 7.12–7.06 (m, 1H), 4.29 (s, 2H), 3.39 (t, J = 6.0 Hz, 2H), 2.83 (t, J = 6.0 Hz, 2H); HRESIMS calcd for $C_{16}H_{14}N_2NaO_2S$ m/z [M + Na]$^+$ 321.0668, found 321.0661; calcd for $C_{16}H_{15}N_2O_2S$ m/z [M + H]$^+$ 299.0849, found 299.0842; HPLC purity 99.5%.

See Supporting Information for details of the syntheses of related compounds **66, 68–71,** and **72** of Table 6 from tetrahydroisoquinoline **96a** and sulfonyl chlorides **103b–e**.

3-(3,4-Dihydroisoquinolin-2(1H)-ylsulfonyl)aniline (67). A solution of the 3-nitro analogue **66** (1.00 g, 3.14 mmol) in a mixture of AcOH (1 mL), DMF (15 mL), EtOH (20 mL), and water (2 mL) was treated at reflux with Fe powder (2.0 g, excess). The mixture was heated for a further hour and then treated with concentrated NH$_4$OH (2 mL), filtered through Celite, and concentrated to a small volume. Dilution with water gave a solid that was recrystallized from EtOAc/petroleum ether to give **67** (0.81 g, 89%); mp 208–209 °C; ^{1}H NMR [(CD$_3$)$_2$SO]: δ 7.23 (t, J = 7.9 Hz, 1H), 7.19–7.07 (m, 4 H), 7.00 (t, J = 1.9 Hz, 1H), 6.89 (d, J = 7.7 Hz, 1H), 6.81 (dd, J = 1.5, 1.0 Hz, 1H), 5.60 (s, 2H), 4.15 (s, 2H), 3.25 (t, J = 5.9 Hz, 2H), 2.86 (t, J = 5.8 Hz, 2H); HRESIMS calcd for $C_{15}H_{16}NaN_2O_2S$ m/z [M + Na]$^+$ 311.0825, found 311.0845; HPLC purity 99.9%.

2-(3-(3,4-Dihydroisoquinolin-2(1H)-ylsulfonyl)phenylamino)-2-oxoacetic Acid (72). A stirred suspension of **67** (400 mg, 1.39 mmol) in a mixture of THF (30 mL) and pyridine (5 mL) was treated dropwise with ethyl 2-chloro-2-oxoacetate (0.20 mL, 179 mmol) at 10 °C. The mixture was stirred at 20 °C for 1 h and then diluted with water (200 mL) and stirred for a further 30 min. The resulting solid was collected and washed with hexane to give ethyl 2-(3-(3,4-dihydroisoquinolin-2(1H)-ylsulfonyl)phenylamino)-2-oxoacetate (**104**) (513 mg, 95%) [mp (EtOAc/petroleum ether) 156–158 °C] which was used directly; ^{1}H NMR [(CD$_3$)$_2$SO]: δ 11.09 (s, 1H), 8.29 (s, 1H), 8.04 (d, J = 7.1 Hz, 1H), 7.68–7.53 (m, 2H), 7.14 (br s, 4H),

4.33 (q, J = 6.8 Hz, 2H), 4.21 (s, 2H), 3.29 (after D_2O exchange, s, 2H), 2.87 (s, 2H), 1.32 (t, J = 6.8 Hz, 3H).

A stirred suspension of **104** (0.25 g, 0.64 mmol) in THF (6 mL) was treated dropwise with a solution of Cs$_2$CO$_3$ (0.23 g, 0.71 mmol) in water (3 mL). The mixture was stirred at 20 °C for 3 h and then diluted with 0.1 H HCl (80 mL). The resulting solid was extracted with dilute NH$_4$OH, and the filtrate was acidified to give a solid. Recrystallization of this from MeOH/water gave **72** (176 mg, 76%); mp 194 °C; ^{1}H NMR [(CD$_3$)$_2$SO]: δ 14.33 (v br s, 1H), 11.06 (s, 1H), 8.33 (t, J = 7.0 Hz, 1H), 8.04 (dt, J = 7.8, 1.7 Hz, 1H), 7.61 (t, J = 7.8 Hz, 1H), 7.57 (dt, J = 7.9, 1.5 Hz, 1H), 7.17–7.08 (m, 4H), 4.20 (2, 2H), 3.28 (after D_2O exchange, t, J = 6.0 Hz, 2H), 2.87 (t, J = 5.9 Hz, 2H); HRESIMS calcd for $C_{17}H_{15}N_2O_5$ m/z [M − 1]$^-$ 359.0707, found 359.0715; HPLC purity 99.7%.

2-((3-(2H-Tetrazol-5-yl)phenyl)sulfonyl)-1,2,3,4-tetrahydroisoqui-noline (74). A mixture of nitrile **65** (269 mg, 0.90 mmol, 1.00 equiv) and NH$_4$Cl (60 mg, 1.13 mmol, 1.25 equiv) in DMF (14 mL) was treated with solid sodium azide (73 mg, 1.13 mmol, 1.25 equiv), and the resulting mixture was stirred at 120 °C for 69 h (method of Nakamura et al.[32]). The reaction mixture was cooled to 20 °C and concentrated to dryness under reduced pressure. Trituration of the resulting orange-brown residue in an ultrasonic bath afforded a pale orange-brown solid, which was reprecipitated from EtOAc/hexanes to give tetrazole **74** (107 mg, 35%) as an amorphous off-white solid; mp 250–251 °C; ^{1}H NMR [(CD$_3$)$_2$SO]: δ 17.07 (br s, 1H), 8.45 (t, J = 1.6 Hz, 1H), 8.33 (dt, J = 7.9, 1.4 Hz, 1H), 8.00 (dt, J = 7.9, 1.4 Hz, 1H), 7.84 (t, J = 7.8 Hz, 1H), 7.12 (m, 4H), 4.29 (s, 2H), 3.39 (t, J = 6.0 Hz, 2H), 2.86 (t, J = 6.0 Hz, 2H); HRESIMS calcd for $C_{16}H_{16}N_5O_2S$ m/z [M + H]$^+$ 342.1019, found 342.1027; HPLC purity 99.5%.

Compounds of Table 6 (Scheme 3B). 3-((3,4-Dihydroisoqui-nolin-2(1H)-yl)sulfonyl)-N-sulfamoylbenzamide (73). A solution of acid **17** (1.80 g, 5.67 mmol, 1.00 equiv) in THF (15 mL) was treated with CDI (2.00 g, 12.33 mmol, 2.17 equiv), and the resulting mixture was stirred for 70 min at 60 °C to give the intermediate imidazolide. The mixture was cooled to 20 °C and treated with sulfamide (1.105 g, 11.502 mmol, 2.028 equiv) for 30 min at 20 °C, and then a solution of DBU (1.72 mL, 11.50 mmol, 2.03 equiv) was added dropwise. After the exotherm, the mixture was stirred at 20 °C for 2.5 h and then diluted with EtOAc (56 mL) and CH$_2$Cl$_2$ (68 mL) and washed with 1 M HCl (68 mL × 2). The combined aqueous layers were extracted with CH$_2$Cl$_2$ (38 mL x 2), and the remaining aqueous suspension was filtered through a pad of Celite to afford an amorphous yellow solid. Reprecipitation of this from EtOAc/hexanes/MeOH furnished **73** (82 mg, unoptimized) as an amorphous white solid; mp 188–189 °C; ^{1}H NMR [(CD$_3$)$_2$SO]: δ 12.25 (s, 1H), 8.36 (t, J = 1.6 Hz, 1H), 8.20 (dt, J = 8.0, 1.3 Hz, 1H), 8.02 (d, J = 7.8 Hz, 1H), 7.74 (t, J = 7.8 Hz, 1H), 7.37 (br s, 2H), 7.18–7.09 (m, 4H), 4.25 (s, 2H), 3.35 (t, J = 6.0 Hz, 2H), 2.85 (t, J = 5.9 Hz, 2H); HRESIMS calcd for $C_{16}H_{17}N_3NaO_5S_2$ m/z [M + Na]$^+$ 418.0502, found 418.0503; HPLC purity 98.7%.

See Supporting Information for details of the syntheses of related compounds **75–82** of Table 6 from the acid chloride of **17** and a variety of known amines.

Compounds of Table 6 (Scheme 3C). 1-(4-(3,4-Dihydroisoqui-nolin-2(1H)-ylsulfonyl)phenyl)pyrrolidin-2-one (83). 2-((4-Iodophenyl)sulfonyl)-1,2,3,4-tetrahydroisoquinoline (**107**) (42 mg, 105 μmol), Pd$_2$dba$_3$ (25 mg, 27 μmol, 0.2 equiv), Xantphos (30 mg, 52 μmol, 0.4 equiv), 2-pyrrolidinone (11 mg, 126 μmol, 1.2 equiv), and Cs$_2$CO$_3$ (52 mg, 160 μmol, 1.5 equiv) were dissolved in dry dioxane (1 mL, 0.1 M) and heated at 100 °C for 18 h. The reaction mixture was cooled to 20 °C, and solvent was removed under reduced pressure. The residue was purified by column flash-chromatography on silica to give **83** (71%); mp 180–181 °C; ^{1}H NMR (CDCl$_3$): δ 7.85–7.80 (m, 4 H), 7.16–7.14 (m, 2 H), 7.17–7.14 (m, 2), 7.14–7.06 (m, 1 H), 7.03–7.01 (m, 1 H), 4.26 (s, 2 H), 3.89 (t, J = 7.20 Hz, 2 H), 3.37 (t, J = 6.00 Hz, 2 H), 2.92 (t, J = 6.00 Hz, 2 H), 2.65 (t, J = 8.00 Hz, 2 H), 2.22 (hept, J = 3.20 Hz, 2 H). HRESIMS m/z [M + H]$^+$ 357.1267; found: 357.1258; [M + Na]$^+$ calculated: 379.1087; found: 379.1088; HPLC purity 99.8%. Anal. Calcd for $C_{19}H_{20}N_2O_3S \cdot 0.5H_2O$: C, H, N.

Compounds of Table 7 (Scheme 4A). *(S)-1-(Naphthalen-2-ylsulfonyl)piperidine-3-carboxylic Acid (84).* Reaction of naphthalene-2-sulfonyl chloride (**106**) and (*S*)-piperidine-3-carboxylic acid (**107a**) by method A gave acid **86** (yield 53%); mp 103−105 °C; ^{1}H NMR [(CD$_3$)$_2$SO]: δ 12.49 (s$_{br}$, 1 H), 8.45 (d, *J* = 1.44 Hz, 1 H), 8.23 (d, *J* = 7.96 Hz, 1 H), 8.17 (d, *J* = 8.72 Hz, 1 H), 8.08 (d, *J* = 14.04 Hz, 1 H), 7.78−7.66 (m, 3 H), 3.60 (dd, *J* = 8.20 Hz, *J* = 2.84 Hz, 1 H), 3.44−3.36 (m, 1 H), 2.60 (t, *J* = 9.88 Hz, 1 H), 2.55−2.45 (m, 2 H), 1.8−1.65 (m, 2 H), 1.57−1.43 (m, 1 H), 1.40−1.28 (m, 1 H) ppm. HRMS (ESI): *m/z* = [M + H]$^+$ calculated: 320.0951; found: 320.0955; [M + Na]$^+$ calculated: 342.0770; found: 342.0777; [M + K]$^+$ calculated: 358.0510; found: 358.0508. HPLC purity 99.6%. Anal. Calcd for C$_{16}$H$_{17}$NO$_4$S: C,H,N.

See Supporting Information for details of the syntheses of related compounds **85−88** of Table 7 from sulfonyl chloride **106** and aminoacids **107b−e**.

Compounds of Table 7 (Scheme 4B). *1-(4′-Chlorobiphenyl-4-ylsulfonyl)piperidine-3-carboxylic acid (89).* Reaction of piperidine-3-carboxylic acid (**108**) and 4′-chlorobiphenyl-4-sulfonyl chloride (**109a**) by method A gave acid **89** (yield 56%); mp 257−260 °C; ^{1}H NMR [(CD$_3$)$_2$SO]: δ 12.51 (s$_{br}$, 1 H), 7.95 (dd, *J* = 6.73 Hz, *J* = 1.81 Hz, 2 H), 7.84−7.76 (m, 4 H), 7.58 (m, 2 H), 3.49 (d, *J* = 8.93 Hz, 1 H), 3.29 (d, *J* = 11.24 Hz, 1 H), 2.60−2.40 (m, 3 H), 1.85−1.78 (m, 1 H), 1.78−1.68 (m, 1 H), 1.58−1.43 (m, 1 H), 1.42−1.30 (m, 1 H) ppm. HRMS (ESI): *m/z* = [M + H]$^+$ calculated: 380.0718; found: 380.0707; [M + Na]$^+$ calculated: 402.0537; found: 402.0529; [M + K]$^+$ calculated: 418.0277; found: 418.0260; HPLC purity 96.5%. Anal. Calcd for C$_{18}$H$_{18}$ClNO$_4$S: C,H,N.

See Supporting Information for details of the syntheses of related compounds **90−94** of Table 7 from **108** and sulfonyl chlorides **109b−f**.

Crystallization and Structure Determination. C-terminal His$_6$-tagged human AKR1C3 was purified following a published procedure,[19] with the incorporation of a final Blue Sepharose 6B step to produce stable, crystallization-grade protein.[33] Two conditions from the PACT premier screen (Molecular Dimensions Ltd.) were found to give highly reproducible, single crystals for the binary complex of AKR1C3 with NADP$^+$: 25% (w/v) PEG1500, 0.1 M PCTP buffer, pH 8.0 (condition C5) and 20% (w/v) PEG3350, 0.2 M sodium acetate (condition E7). Sitting drop experiments were set up on a Mosquito crystallization robot (TTP Labtech) using drops comprising 800 nL of protein (20 mg·mL^{-1}) + 800 nL of reservoir solution at 16 °C. Crystals with a rod shaped morphology appeared within 3 days. Crystals were soaked with 5 mM compound **79** or compound **85** for 3 days and were subsequently flash frozen in liquid nitrogen using 20% ethylene glycol + 5 mM compound in reservoir solution as cryoprotectant. Crystals for AKR1C3 in complex with compound **17** were obtained by incubating protein at 20 mg·mL^{-1} overnight in the presence of 2.4 mM compound prior to setting up coarse screen cocrystallization experiments. Drops comprising 250 nL of protein + 250 nL of reservoir solution were set up at 16C. Crystals with a rodlike morphology grew from the PACT premier screen condition, E4 (0.2 M potassium thiocyanate, 20% (w/v) PEG3350). These crystals were cryopRotected with 20% ethylene glycol + 5 mM compound in reservoir solution prior to flash freezing in liquid nitrogen.

Data were collected at 100 K on a Rigaku Micromax-007 HF X-ray generator with Varimax HF Optics and a Rigaku Saturn 944 CCD detector. These data were processed using the program StructureeStudio (Rigaku). The structures were solved by molecular replacement using the program PHASER[34] and the structure of AKR1C3+NADP$^+$ (PDB code = 2FGB) as the search model. The models were rebuilt using COOT[35] and refined using REFMAC5.[36] The refinement statistics are summarized in S2 (see Supporting Information). The coordinates and diffraction amplitudes have been deposited in the Protein Data Bank with accession codes 4FAM (**17**), 4FAL (**80**), and 4FA3 (**86**).

Energy Minimization. The structure for flufenamic acid bound to AKR1C3 was obtained from the Protein Data Bank, code 1S2C, and was prepared along with the structures determined here using SYBYL8.0.3 (Tripos, St. Louis, MO). Preparation included stripping water and addition of hydrogens followed by visual inspection. Minimization of inhibitors within the AKR1C3 active site was performed with SZYBKI v1.5.1 (OpenEye Scientific Software, Santa Fe, NM) using the conjugate gradient method until convergence at 0.05 kcal/(mol·A). Only the protein polar hydrogens within 8 Å were allowed to optimize along with the ligand. The MMFF94s potential function was used with the exact analytical VdW potential, protein dielectric set at 2, the Poisson−Boltzmann solvent model, and the VdW protein−ligand interaction sphere at 18.0 Å; all frozen terms were used in the single-point calculation. All other settings were used at default values. Where the ligand was minimized in the absence of protein, the MMFF94s potential function was used with the exact analytical VdW potential, and the Poisson−Boltzmann solvent model with a solvent dielectric of 1 and the cavity salvation term at 0.025. The conjugate gradient method was used until convergence at 0.05 kcal/(mol·A); all other settings were used at default values.

COX Assays. (carried out by GVK Biosciences Ltd., Biology, 28A, IDA Nacharam, Hyderabad 500 076 India: www.gvkbio.com)

COX 1: Human whole blood collected by venipuncture into heparin (60 U/mL) tubes was half diluted into RPMI medium (without FBS) and treated with test compound (10 μM) for 1 h at 37 °C in 5% CO$_2$ in a 96-well plate. Calcium ionophore A23187 (50 μM) was added, and the plates were incubated for another 30 min under the same conditions and then centrifuged for 10 min at 250G/4 °C, and supernatant was collected and frozen at −80 °C for ELISA.

COX 2: Heparinized human whole blood was treated with aspirin (12 μg/mL) to inactivate COX 1 and then incubated for 6 h, diluted 2-fold, and treated with test compound (10 μM) as above. LPS was then added (final concentration 10 μg/mL), and the plates were incubated for another 18 h and then centrifuged, and supernatant was collected as above.

The supernatants were then assayed for thromboxane B2 (TBX2) using an Assay Designs (Enzo Life Sciences Ltd.) immunoassay kit.

Production of Enzyme Expression Vectors. The AKR1C3 gene was amplified from an IMAGE cDNA clone (3682448; Source Bioscience, Nottingham, U.K.) by PCR using forward (AACCTTCA-TATGGATTCCAAACACCAG) and reverse (AACCTTCTCGAGT-TAATATTCATCTGAAT) primers that introduced an *Nde*I restriction site overlapping the start codon and a downstream *Xho*I site before the stop codon. The digested fragment was ligated into a pET28a plasmid vector (Merck Chemicals, Nottingham, U.K.), and the nucleotide sequence of the cloned AKR1C3 gene was confirmed by DNA sequencing. The expression plasmid incorporated an N-terminal His-tag to aid purification. AKR1C1, AKR1C2, and AKR1C4 expression vectors were a gift from Dr Chris Bunce, University of Birmingham.

Expression and Purification of Recombinant His-Tagged Enzyme. The AKR1C enzyme constructs were transformed in *Escherichia coli* BL21 (DE3) cells (Invitrogen, Paisley, Scotland, U.K.) and plated on L-agar supplemented with 30 μg/mL kanamycin. Colonies were cultured in 100 mL L-broth with 30 μg/mL kanamycin for 6 h at 37 °C with shaking at 220 rpm. Cultures were expanded by diluting 1:500 in Terrific broth supplemented with 30 μg/mL kanamycin and were grown at 37 °C for 8 h with shaking at 160 rpm. Cells were harvested by centrifugation at 10000*g* for 30 min at 4 °C.

The cell pellet was resuspended in 50 mM potassium phosphate buffer (pH = 7.2) with protease inhibitor cocktail (Roche Diagnostics Ltd., Burgess Hill, West Sussex, U.K.), lysed by sonication on ice and centrifuged at 20000*g* for 45 min at 4 °C. Protein was purified using an AKTA FPLC (GE Healthcare, Chalfont St Giles, Buckinghamshire, U.K.), by loading the cell supernatant onto an IMAC column charged with Ni^{2+} using a P960 pump at 4 mL/min. Unbound protein was washed with 50 mM potassium phosphate buffer (pH = 7.2) and 5 mM imidazole buffer at 1 mL/min. The recombinant protein was eluted using a linear 5−500 mM imidazole gradient in 50 mM potassium phosphate buffer (pH = 7.2) at 1 mL/min. Pooled fractions containing overexpressed enzyme, as determined by SDS-PAGE, were dialyzed against 50 mM potassium phosphate buffer (pH = 7.2) and 1

mM DTT at 4 °C for a minimum of 4 h to remove imidazole. The protein was concentrated on a Vivaspin concentrator (GE Healthcare) with a 10000 M_w cutoff for size exclusion chromatography on a 26/60 Superdex 200 column (GE Healthcare) at 0.5 mL/min in 50 mM potassium phosphate buffer (pH = 7.2), 1 mM DTT, and 150 mM NaCl. The expression of purified N-terminal His-tagged recombinant enzyme was confirmed by SDS-PAGE.

Measurement of AKR1C Enzyme Activity. A competitive fluorescence assay was used to measure AKR1C enzyme activity, where a nonfluorescent ketone probe (probe 5)[37] selective for the AKR1C enzyme isoforms is reduced to a fluorescent alcohol in the presence of AKR1C enzyme and NADPH. Briefly, purified protein (2 μg/mL AKR1C1, 1 μg/mL AKR1C2, 2 μg/mL AKR1C3, and 5 μg/mL AKR1C4) were incubated with 40 μM probe 5, test compounds, and 50 μM NADPH in an assay buffer of 10 mM MOPS (pH = 7.2), 130 mM NaCl, 1 mM DTT, and 0.01% Triton-X-100 for 1 h at 37 °C. The reaction was stopped by addition of 35 mM NaOH, and fluorescence was read in a SpectraMax M2 microplate reader (Molecular Devices, Sunnyvale, CA, USA) at excitation/emission wavelengths of 420/510 nM. The compounds and known AKR1C3 inhibitors (flufenamic acid, indomethacin, naproxen, meclofenamic acid, S(+)-ibuprofen and flurbiprofen; Sigma-Aldrich, Auckland, New Zealand) were tested at multiple concentrations between 0.1 nM and 100 μM in 2% DMSO to generate AKR1C enzyme inhibition data. Compound IC_{50} values were calculated by fitting the inhibition data to a four-parameter logistic sigmoidal dose–response curve using Prism 5.02 (GraphPad, La Jolla, CA, USA).

Inhibition of Cellular AKR1C3 Activity. AKR1C3 activity was determined in HCT-116 cells engineered to overexpress AKR1C3 by measuring the major metabolite (PR-104H) of PR-104A 2-electron reduction under aerobic conditions, a reaction catalyzed selectively by AKR1C3.[6] The synthesis of PR-104A, PR-104H, and tetradeuterated PR-104H,[38,39] the transfection of the HCT-116/AKR1C3 cell line,[6] and the measurement of PR-104H by LC-MS/MS have been described previously.[40] The compounds were administered 2 h prior to 100 μM PR-104A at multiple concentrations between 1 nM and 3 μM. PR-104H formation was quantitated against a PR-104H standard curve ranging from 1 to 1000 nM. Compound IC_{50} values were calculated from four-parameter logistic sigmoidal dose–response curves that were fitted to the inhibition data using Prism 5.02. Representative compounds were tested over repeat assays to ensure assay reproducibility.

■ ASSOCIATED CONTENT

Ⓢ Supporting Information

Additional experimental procedures and characterizations for the compounds in Tables 2, 3, and 5–7, as well as combustion analytical data and the structures of probe 5 and PR-104A. This material is available free of charge via the Internet at http://pubs.acs.org.

■ AUTHOR INFORMATION

Corresponding Author

*Tel.: +64 9 923 6144. Fax: +64 9 3737502. E-mail address: b.denny@auckland.ac.nz.

Notes

The authors declare no competing financial interest.

■ ACKNOWLEDGMENTS

■ ABBREVIATIONS

AKR, aldo-keto reductase; COX, cyclooxygenase; APCI, low-resolution atmospheric pressure chemical ionization mass spectrometry; DMF, dimethylformamide; HREIMS, HRFABMS, HRESIMS and HRAPCIMS, high-resolution electron impact, fast atom bombardment, electrospray ionization, and atmospheric pressure chemical ionization mass spectrometry; NADP, nicotinamide adenine dinucleotide phosphate; NSAID, nonsteroidal anti-inflammatory; PBD, protein databank; THF, tetrahydrofuran

■ REFERENCES

(1) Barski, O. A.; Tipparaju, S. M.; Bhatnagar, A. The aldo-keto reductase superfamily and its role in drug metabolism and detoxification. *Drug Met. Rev.* **2008**, *40*, 553–624.

(2) Penning, T. M.; Burczynski, M. E.; Jez, J. M.; Hung, C.-F.; Lin, H.-K.; Ma, H.; Moore, M.; Palackal, N.; Ratnam, K. Human 3α-hydroxysteroid dehydrogenase isoforms (AKR1C1−AKR1C4) of the aldo-keto reductase superfamily: functional plasticity and tissue distribution reveals roles in the inactivation and formation of male and female sex hormones. *Biochem. J.* **2000**, *351*, 67–77.

(3) Komoto, J.; Yamada, T.; Watanabe, K.; Takusagawa, F. Crystal structure of human prostaglandin F synthase (AKR1C3). *Biochemistry* **2004**, *43*, 2188–2198.

(4) Desmond, J. C.; Mountford, J. C.; Drayson, M. T.; Walker, E. A.; Hewison, M.; Ride, J. P.; Luong, Q. T.; Hayden, R. E.; Vanin, E. F.; Bunce, C. M. The aldo-keto reductase AKR1C3 is a novel suppressor of cell differentiation that provides a plausible target for the non-cyclooxygenase-dependent antineoplastic actions of nonsteroidal anti-inflammatory drugs. *Cancer Res.* **2003**, *63*, 505–512.

(5) Novotna, R.; Wsol, V.; Xiong, G.; Maser, E.. Inactivation of the anticancer drugs doxorubicin and oracin by aldo-keto reductase (AKR)1C3. *Toxicol. Lett.* **2008**, *181*, 1–6.

(6) Guise, C. P.; Abbattista, M. R.; Singleton, R. S.; Holford, S. D.; Connolly, J.; Dachs, G. U.; Fox, S. B.; Pollock, R.; Harvey, J.; Guilford, P.; Donate, F.; Wilson, W. R.; Patterson, A. V. The bioreductive prodrug PR-104A is activated under aerobic conditions by human aldo-keto reductase 1C3. *Cancer Res.* **2010**, *70*, 1573–1584.

(7) Steckelbroeck, S.; Jin, Y.; Gopishetty, S.; Oyesanmi, B.; Penning, T. M. Human cytosolic 3α-hydroxysteroid dehydrogenases of the aldo−keto reductase superfamily display significant 3β-hydroxysteroid dehydrogenase activity: implications for steroid hormone metabolism and action. *J. Biol. Chem.* **2003**, *279*, 10784–10795.

(8) Penning, T. M.; Steckelbroeck, S.; Bauman, D. R.; Miller, M. W.; Jin, Y.; Peehl, D. M.; Fung, K. M.; Lin, H. K. Aldo-keto reductase AKR1C3: role in prostate disease and the development of specific inhibitors. *Mol. Cell. Endocrinol.* **2006**, *248* (1−2), 182–191.

(9) Brozic, P.; Turk, S.; Rizner, T. L.; Gobec, S. Inhibitors of aldo-keto reductases AKR1C1-AKR1C4. *Curr. Med. Chem.* **2011**, *18*, 2554–2565.

(10) Byrns, M. C.; Jin, Y.; Penning, T. M. Inhibitors of type 5 17β-hydroxysteroid dehydrogenase (AKR1C3): Overview and structural insight. *J. Steroid Biochem. Mol. Biol.* **2011**, *125*, 95–104.

(11) Davies, N. J.; Hayden, R. E.; Simpson, P. J.; Birtwistle, J.; Mayer, K.; Ride, J. P.; Bunce, C. M. AKR1C isoforms represent a novel cellular target for jasmonates alongside their mitochondrial-mediated effects. *Cancer Res.* **2009**, *69*, 4769–4775.

(12) Stefane, B.; Brozic, P.; Vehovc, M.; Rizner, T. L.; Gobec, S. New cyclopentane derivatives as inhibitors of steroid metabolizing enzymes AKR1C1 and AKR1C3. *Eur. J. Med. Chem.* **2009**, *44*, 2563–2571.

(13) Adeniji, A. O.; Twenter, B. M.; Byrns, M. C.; Jin, Y.; Chen, M.; Winkler, J. D.; Penning, T. M. Development of potent and selective inhibitors of aldo-keto reductase 1C3 (type 5 17β-hydroxysteroid dehydrogenase) based on N-phenyl-aminobenzoates and their structure-activity relationships. *J. Med. Chem.* **2012**, *55*, 2311–2323.

(14) Komoto, J.; Yamada, T.; Watanabe, K.; Takusagawa, F. Crystal structure of human prostaglandin F synthase (AKR1C3). *Biochemistry* **2004**, *43*, 2188−2198.

(15) Skarydova, L.; Zivna, L.; Xiong, G.; Maser, E.; Wsol, V. AKR1C3 as a potential target for the inhibitory effect of dietary flavonoids. *Chem.-Biol. Interact.* **2009**, *178*, 138−144.

(16) Endo, S.; Matsunaga, T.; Kanamori, A.; Otsuji, Y.; Nagai, H.; Sundaram, K.; El-Kabbani, O.; Toyooka, N.; Ohta, S.; Hara, A. Selective inhibition of human type-5 17β-hydroxysteroid dehydrogenase (AKR1C3) by baccharin, a component of Brazilian propolis. *J. Nat. Prod.* **2012**, *75*, 716−721.

(17) Adeniji, A. O.; Twenter, B. M.; Byrns, M. C.; Jin, Y.; Winkler, J. D.; Penning, T. M. Discovery of substituted 3-(phenylamino)benzoic acids as potent and selective inhibitors of type 5 17β-hydroxysteroid dehydrogenase (AKR1C3). *Bioorg. Med. Chem. Lett.* **2011**, *21*, 1464−1468.

(18) Xu, X. C. Cox-2 inhibitors in cancer treatment and prevention, a recent development. *Anti-Cancer Drugs* **2002**, *13*, 127−137.

(19) Lovering, A. L.; Ride, J. P.; Bunce, C. M.; Desmond, J. C.; Cummings, S. M.; White, S. A. Crystal structures of prostaglandin D2 11-ketoreductase (AKR1C3) in complex with the nonsteroidal anti-inflammatory drugs flufenamic acid and indomethacin. *Cancer Res.* **2004**, *64*, 1802−1810.

(20) Byrns, M. C.; Penning, T. M. Type 5 17β-hydroxysteroid dehydrogenase/prostaglandin F synthase (AKR1C3): Role in breast cancer and inhibition by non-steroidal anti-inflammatory drug analogs. *Chem.-Biol. Interact.* **2009**, *178*, 221−227.

(21) Kakefuda, A.; Kondoh, Y.; Hirano, M.; Kamikawa, A.; Enjo, K.; Furutani, T. Benzimidazole derivatives. WO 2009/014150 A1, published June 29th, 2009.

(22) Shearer, B. G.; Patel, H. S.; Billin, A. N.; Way, J. M.; Winegar, D. A.; Lambert, M. H.; Xu, R. X.; Leesnitzer, L. M.; Merrihew, R. V.; Huet, S.; Willson, T. M. Discovery of a novel class of PPARδ partial agonists. *Bioorg. Med. Chem. Lett.* **2008**, *18*, 5018−5022.

(23) Isabel, E.; Black, W. C.; Bayly, C. I.; Grimm, E. L.; Janes, M. K.; McKay, D. J.; Nicholson, D. W.; Rasper, D. M.; Renaud, J.; Roy, S.; Tam, J.; Thornberry, N. A.; Vaillancourt, J. P.; Xanthoudakis, S.; Zamboni, R. Nicotinyl aspartyl ketones as inhibitors of caspase-3. *Bioorg. Med. Chem. Lett.* **2003**, *13*, 2137−2140.

(24) Black, C.; Grimm, E. L.; Isabel, E.; Renaud, J. Nicotinyl aspartyl ketones as inhibitors of caspase-3. Patent WO 01/27085 A1, 2001.

(25) Pu, Y.-M.; Christesen, A.; Ku, Y.-Y. A simple and highly effective oxidative chlorination protocol for the preparation of arenesulfonyl chlorides. *Tetrahedron Lett.* **2010**, *51*, 418.

(26) Byrns, M. C.; Steckelbroeck, S.; Penning, T. M. An indomethacin analogue, *N*-(4-chlorobenzoyl)-melatonin, is a selective inhibitor of aldo-keto reductase 1C3 (type 2 3α-HSD, type 5 17β-HSD, and prostaglandin F synthase), a potential target for the treatment of hormone dependent and hormone independent malignancies. *Biochem. Pharmacol.* **2008**, *75*, 484−493.

(27) Orazi, O. O.; Corral, R. A.; Giaccio, H. Synthesis of fused heterocycles: 1,2,3,4-tetrahydroisoquinolines and ring homologues *via* sulphonamidomethylation. *J. Chem. Soc., Perkin Trans. 1* **1986**, 1977.

(28) Feng, D.-J.; Wang, P.; Li, X.-Q.; Li, Z.-T. Self-assembly of hydrazide-based heterodimers driven by hydrogen bonding and donor-acceptor interaction. *Chin. J. Chem.* **2006**, *24*, 1200−1208.

(29) Myers, A. G.; Dragovich, P. S. Synthesis of functionalises enynes by palladium/copper-catalyzed coupling reactions of acetylenes with (Z)-2,3-dibromopropenoic acid ethyl ester: (Z)-2-bromo-5-(trimethylsilyl)-2-penten-4-ynoic acid ethyl ester. *Org. Synth.* **1995**, *72*, 104−111.

(30) Nicolaou, K. C.; Tang, Y.; Wang, J. Total synthesis of sporolide B. *Angew. Chem., Int. Ed.* **2009**, *48*, 3449−3453.

(31) Gu, Z.; Li, Z.; Liu, Z.; Wang, Y.; Liu, C.; Xiang, J. Simple, efficient copper-free Sonogashira coupling of haloaryl carboxylic acids or unactivated aryl bromides with terminal alkynes. *Catal. Commun.* **2008**, *9*, 2154−2157.

(32) Nakamura, T.; Sato, M.; Kakinuma, H.; Miyata, N.; Taniguchi, K.; Bando, K.; Koda, A.; Kameo, K. Pyrazole and isoxazole derivatives as new, potent, and selective 20-hydroxy-5,8.11,14-eicosatetraenoic acid synthase inhibitors. *J. Med. Chem.* **2003**, *46*, 5416−5427.

(33) Zhou, M.; Wei Qiu, W.; Chang, H.-J.; Gangloff, A.; Lin, S.-X. Purification, crystallization and preliminary X-ray diffraction results of human 17β-hydroxysteroid dehydrogenase type 5. *Acta Crystallogr.* **2002**, *D58*, 1048−1050.

(34) McCoy, A. J.; Grosse-Kunstleve, R. W.; Adams, P. D.; Winn, M. D.; Storoni, L. C.; Read, R. J. Phaser crystallographic software. *J. Appl. Crystallogr.* **2007**, *40*, 658−674.

(35) Emsley, P.; Cowtan, K. Coot: model-building tools for molecular graphics. *Acta Crystallogr.* **2004**, *D60*, 2126−2132.

(36) Murshudov, G. N.; Lebedev, A.; Vagin, A. A.; Wilson, K. S.; Dodson, E. J. Efficient anisotropic refinement of Macromolecular structures using FFT. *Acta Crystallogr.* **1999**, *D55*, 247−255.

(37) Yee, D. J.; Balsanek, V.; Sames, D. New tools for molecular imaging of redox metabolism: development of a fluorogenic probe for 3α-hydroxysteroid dehydrogenases. *J. Am. Chem. Soc.* **2004**, *126*, 2282−2283.

(38) Yang, S.; Atwell, G. J.; Denny, W. A. Synthesis of asymmetric halomesylate mustards with aziridineethanol/alkali metal halides: application to an improved synthesis of the hypoxia prodrug PR-104. *Tetrahedron* **2007**, *63*, 5470−5476.

(39) Atwell, G. J.; Denny, W. A. Synthesis of ³H- and ²H4-labelled versions of the hypoxia-activated pre-prodrug 2-[(2-bromoethyl)-2,4-dinitro-6-[[[2-(phosphonooxy)ethyl]amino] carbonyl]anilino]ethyl methanesulfonate (PR-104). *J. Labelled Compd. Radiopharm.* **2007**, *50*, 7−12.

(40) Singleton, R. S.; Guise, C. P.; Ferry, D. M.; Pullen, S. M.; Dorie, M. J.; Brown, J. M.; Patterson, A. V.; Wilson, W. R. DNA cross-links in human tumor cells exposed to the prodrug PR-104A: relationships to hypoxia, bioreductive metabolism, and cytotoxicity. *Cancer Res.* **2009**, *69*, 3884−3891.